July 1999 • NREL/TP-500-25950

Technical Report

Unsteady Aerodynamics Experiment Phases II–IV Test Configurations and Available Data Campaigns

D.A. Simms, M.M. Hand,
L.J. Fingersh, D.W. Jager

National Renewable Energy Laboratory

1617 Cole Boulevard
Golden, Colorado 80401-3393

NREL is a U.S. Department of Energy Laboratory
Operated by Midwest Research Institute • Battelle • Bechtel

Contract No. DE-AC36-98-GO10337

July 1999 • NREL/TP-500-25950

Unsteady Aerodynamics Experiment Phases II–IV Test Configurations and Available Data Campaigns

D.A. Simms, M.M. Hand,
L.J. Fingersh, D.W. Jager

Prepared under Task No. WE901110

National Renewable Energy Laboratory

1617 Cole Boulevard
Golden, Colorado 80401-3393

NREL is a U.S. Department of Energy Laboratory
Operated by Midwest Research Institute • Battelle • Bechtel

Contract No. DE-AC36-98-GO10337

Acknowledgements

This work was supported by the U.S. Department of Energy under contract number DE-AC36-98-GO10337.

Available to DOE and DOE contractors from:
Office of Scientific and Technical Information (OSTI)
P.O. Box 62
Oak Ridge, TN 37831
Prices available by calling 423-576-8401

Available to the public from:
National Technical Information Service (NTIS)
U.S. Department of Commerce
5285 Port Royal Road
Springfield, VA 22161
703-605-6000 or 800-553-6847
or
DOE Information Bridge
http://www.doe.gov/bridge/home.html

Printed on paper containing at least 50% wastepaper, including 20% postconsumer waste

Table of Contents

List of Figures

List of Figures (continued)

List of Tables

INTRODUCTION

The main objective of the Unsteady Aerodynamics Experiment is to provide information needed to quantify the full-scale three-dimensional aerodynamic behavior of horizontal axis wind turbines. To accomplish this, an experimental wind turbine configured to meet specific research objectives was assembled and operated at the National Renewable Energy Laboratory (NREL). The turbine was instrumented to characterize rotating blade aerodynamic performance, machine structural responses, and atmospheric inflow conditions. Comprehensive tests were conducted with the turbine operating in an outdoor field environment under diverse conditions. Resulting data are used to validate aerodynamic and structural dynamics models which are an important part of wind turbine design and engineering codes. Improvements in these models are needed to better characterize aerodynamic response in both the steady-state post-stall and dynamic stall regimes.

Much of the effort in the earlier phase of the Unsteady Aerodynamics Experiment focused on developing required data acquisition systems. Complex instrumentation and equipment was needed to meet stringent data requirements while operating under the harsh environmental conditions of a wind turbine rotor. Once the data systems were developed, subsequent phases of experiments were then conducted to collect data for use in answering specific research questions. A description of the experiment configuration used during Phases II - IV of the experiment is contained in this report.

Background

Test results from previous phases of the Unsteady Aerodynamics Experiment have shown that wind turbines undergo complex aerodynamic reactions when operating in typical atmospheric conditions. All wind turbine design codes are based on aerodynamic forces derived from steady 2-D wind tunnel airfoil test results. Blade designs are developed assuming steady loading optimization principles. While these design codes produce accurate predictions on average, instantaneous loads and peak power predictions are often incorrect. For horizontal axis wind turbines, these principles are accurate for low to moderate wind speeds, provided that the inflow remains constant. In reality, the inflow conditions exhibit an extremely complex and dynamic nature. Factors such as atmospheric turbulence, shear across the rotor plane, and blade passage through the tower wake all contribute to constantly changing aerodynamic forces that do not obey steady principles. Resulting unsteady aerodynamic forces can be significantly greater than steady forces. These increased fluctuating forces lead to greater dynamic turbine structural responses and high fatigue stresses. With the trend toward lightweight flexible turbines, unsteady aerodynamic loading has become an even more important consideration in predicting dynamic turbine responses.

In order to bridge this gap between the 3-D, unsteady operating environment and the 2-D, steady design environment, NREL implemented the Unsteady Aerodynamics Experiment measurement program designed to obtain experimental data from the 3-D field environment. Measurements needed to quantify the 3-D effects of field operation include meteorological data, loads, local flow angles and blade surface pressures. Meteorological instrumentation was configured to obtain wind speed, wind direction and atmospheric stability measurements upwind of the turbine. Loads, such as power production, low-speed shaft bending and torque, blade root bending, and tower motion, were obtained using various power transducers, accelerometers, and strain gages.

Two devices were used to obtain local flow characteristics in front of one of the three blades. A flag assembly measured local flow angles during the earlier phases of the experiment, and 5-hole differential pressure probes were implemented in the last phase of the experiment to improve the dynamic response of the local flow angle measurement. Lastly, blade surface pressures were measured at one blade span location initially, but the measurements were extended to five span locations as the experiment progressed. In addition to various measurement capabilities, two blade designs were tested. A constant-chord zero-twist blade set was used in earlier phases of testing. A constant-chord optimally twisted blade set was used in later phases. Future tests are planned for a tapered and twisted blade set.

The Unsteady Aerodynamics Experiment was begun in 1987 (it was initially called the "Combined Experiment") and has been implemented in four phases to date. Phase I planning began in 1987 and resulted in valuable knowledge and experience with these types of measurements (Butterfield et al. 1992). The instrumentation configuration that resulted in Phase I was used to obtain the Phase II data in the spring of 1989. Untwisted blades were used again in Phase II, and the pressure instrumentation was expanded from one to four span locations. Optimally twisted blades were designed for Phase III of the project which began in 1993 and resulted in data sets in early 1995. The fourth phase, initiated in late 1995, also used the twisted blades but the flow angle measurements were improved. The significant differences between the Phase II, Phase III, and Phase IV configurations are described in Table 1 below. This report follows the Phase I final report (Butterfield et al. 1992) to explain the evolution of these measurements from Phase II through Phase IV.

Table 1. Unsteady Aerodynamics Experiment Configuration Differences

	Phase II	Phase III	Phase IV
Dates for data collection	4/25/89 - 7/25/92	4/7/95 -6/6/95	4/3/96 - 5/18/96 and 4/29/97 - 5/7/97
Blades	Untwisted	Twisted	Twisted
Local flow angle (LFA) measurement device	Flag	Flag, 5-Hole Probe (test)	5-Hole Probe
Span locations instrumented with LFA sensors	4	5	5
Span locations instrumented with full-chord pressure taps	4	5	5
Span locations instrumented with pairs of pressure taps	6	10	10
Azimuth angle measurements and RPM calculation	Poor	Good	Good
Meteorological instrumentation	Vertical Plane Array	Horizontal and Vertical Shear	Horizontal and Vertical Shear
Blade root strain gages	Yes	Yes	Yes
Blade strain gages	Yes	Yes	No
Blade tip and nacelle accelerometers	No	Yes	Yes
Selections of data during which yaw brake engaged	Yes	No	Yes
Campaign duration	5 minutes	10 minutes	10 minutes
Boom extension and camera mounted on hub; tufts on suction side of instrumented blade	Yes	No	Yes
Video	Yes	No	Yes

	Phase II	Phase III	Phase IV
Pitch angles (blade tip)	12°	3°, -3°, 8°	3°, -3°, 8°, 12°, -9°
File naming conventions: • **parked#, and d4pb###: Rotor brake engaged with instrumented blade at either 0° or 180° azimuth.** • **slwrot# and d4sr###: Blades feathered with rotor slowly rotating.** • **d4pp###: 'pp' indicates pitch angle** • **# indicates numerical order in which data collected**	d6511, d6512, d6521, d6522, d6611,…,d7521, d7522	data1-data19 parked1, parked2, slwrot1, slwrot2	data20-data112, slwrot4, slwrot5 d403001-d403039, d408001-d408012, d4m3001-d4m3012, d4pb001-d4pb009, d4sr001, d412001, d4m9001

This report is intended to provide the reader with information regarding the variations between phases of data collection. The instrumentation used in Phase II was presented by Butterfield et al. (1992), and is summarized in this report. Prior to Phase III, most of the instrumentation was replaced with newer components. The tables in the body of the report that describe the channels collected by the data system are based upon the header files that accompany each data campaign. Appendix A contains information detailing the turbine configuration differences between Phases II, III, and IV that could be used to develop models. Detailed descriptions and figures of each component of instrumentation used during Phases III and IV are included in Appendix B. Flow charts illustrate the complete signal path from the measurement source to the resulting data file. Calibration procedures are presented for each instrument. Data processing procedures and the associated input files are described in Appendix B as well. Appendix C contains manufacturer specifications for the instrumentation components summarized in two tables: one for Phase II and one for Phases III and IV. General atmospheric and turbine conditions are summarized in Appendix D for each phase of the experiment. Instrumentation failures and observations made during data collection are noted.

Test Facility Description

Location

All atmospheric testing was conducted at NREL's National Wind Technology Center located 10 miles north of Golden, Colorado. Winter winds are dominant at this site from a prevailing direction of 292° from true north. Although the local terrain is flat with grassy vegetation extending over 0.8 km upwind, the site is situated about 5 km from the base of the Rocky Mountains which are located directly upwind. The wind turbine site was unobstructed by other wind turbines or structures.

Test Turbine

The Unsteady Aerodynamics Experiment test turbine is a modified Grumman Wind Stream 33. It is a 10-m diameter, three-bladed, downwind, free-yaw turbine equipped with full-span pitch capability that can be manually controlled during the testing to provide fixed-pitch (stall-controlled) operation at any pitch angle desired. The turbine is supported on a guyed-pole tower, 0.4064 m in diameter, that is equipped with a hinged base and gin pole to allow it to be tilted down easily. An electric winch is used to lower and raise the system during installation. A manually operated yaw brake was added to allow fixed-yaw operation at arbitrary yaw positions.

This yaw-retention system has a strain-gaged link that measured yaw moments in Phase II and Phase IV. A mechanical caliper rotor brake system that could be operated manually from the control shed was also added. This feature was used to obtain data with the instrumented blade parked either behind the tower or at the top of the rotational cycle. A complete listing of turbine specifications may be found in Appendix A.

The drive train, pictured in Figure 1, is similar to the original Grumman configuration. The rotor operates at a nominal 72 RPM. Low-speed shaft torque is transferred through a 25.1:1 gearbox ratio to the high-speed shaft that is connected to the 20-kW induction generator. The inertia of the Phase IV rotor (twisted blades, instrumentation boxes, boom, hub, and camera) was determined by measuring low-speed shaft torque, power, and rotational speed during turbine startup. An estimate of drive train (low-speed shaft, gearbox, and high-speed shaft) stiffness was also obtained from this test. The inertia of the entire rotating system (rotor and drive train) was measured with a pendulum test. Data collected during operation of the instrumented turbine provided measurements of the generator slip and total efficiency of the drive train. The machine description in Appendix A lists all of these results.

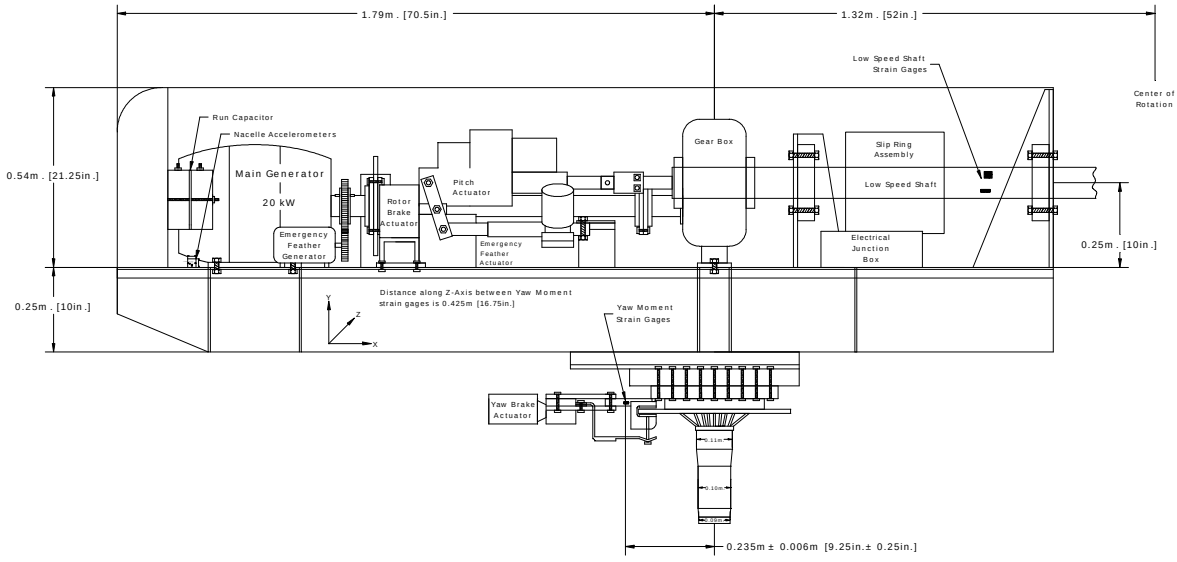

Figure 1. Drive-train configuration.

The most significant configuration change to the original Grumman turbine was the blade design. The NREL S809 airfoil replaced the original Grumman airfoil. The S809 airfoil was developed by Airfoils, Inc., under contract to NREL (Somers 1997). It was optimized to improve wind energy power production and is insensitive to leading edge roughness. The S809 airfoil has a well-documented wind tunnel data base that included pressure distributions, separation boundary locations, drag data, and flow-visualization data (Somers 1997, Butterfield et al. 1992). This airfoil was used in both the untwisted and twisted blade configurations which are pictured in Figures 2 and 3, respectively.

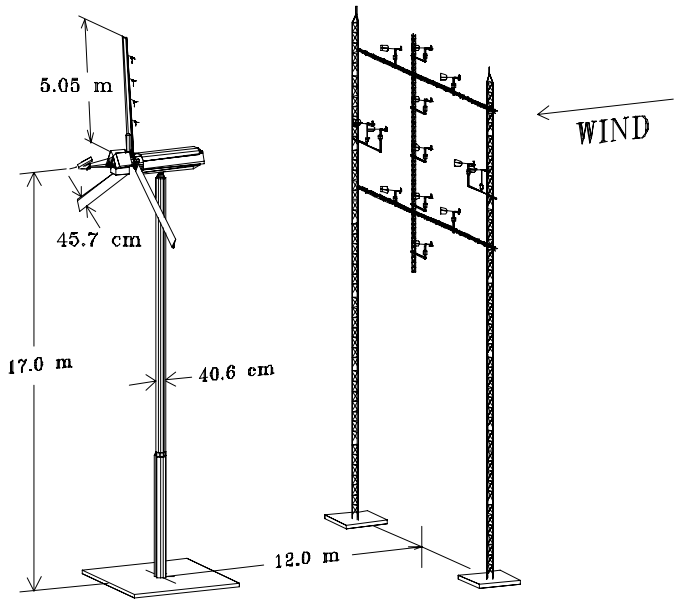

Figure 2. Phase II test configuration. The prevailing wind direction is 292° from true north.

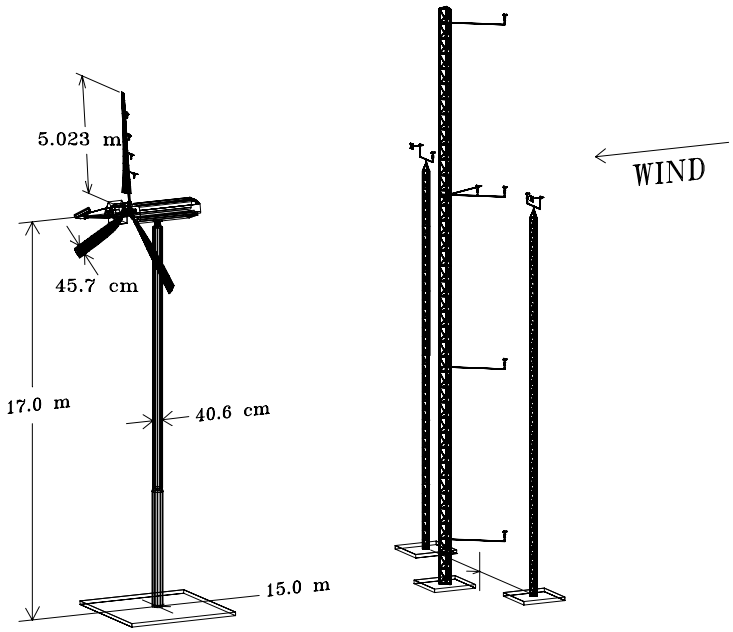

Figure 3. Phase III and Phase IV test configuration. The prevailing wind direction is 292° from true north.

The untwisted and twisted blades were similar in design and fabrication. Both had a constant 0.457-m chord, and a planform view of the blades is shown in Figure 4. The intent in the design of the twisted blades was to maintain a constant angle of attack along the span of the blade at a wind speed of 8 m/s (Simms, Fingersh, and Butterfield 1995). The twist distribution of the blades used in Phases III and IV is listed in Appendix A and shown in Figure 5. The root thickness and airfoil distribution of the twisted blades were nearly identical to that of the untwisted blades with the spar enlargement extending to 25% span instead of 30% span. Both

sets of blades were fiberglass/epoxy composite, but the spar in the twisted blades was carbon fiber as opposed to the fiberglass/epoxy spar used in the untwisted blades. The blades were designed to be stiff to mitigate aeroelastic blade responses. The dynamic characteristics of the blades were tailored to avoid coalescence of rotor harmonics with flap-wise, edge-wise, and torsional natural frequencies. To minimize the possibility of aeroelastic instabilities, the mass and elastic axes were aligned with the aerodynamic axis. The instrumented blade was painted black to contrast with the white tufts that were used for flow visualization. The pitch shaft on which the blades are mounted is less stiff than the inboard sections of the blade, and most of the flap deflection occurs in this region. For this reason, the pitch shaft must be included in a blade or hub model and is included with the estimated blade mass and stiffness distributions in Appendix A.

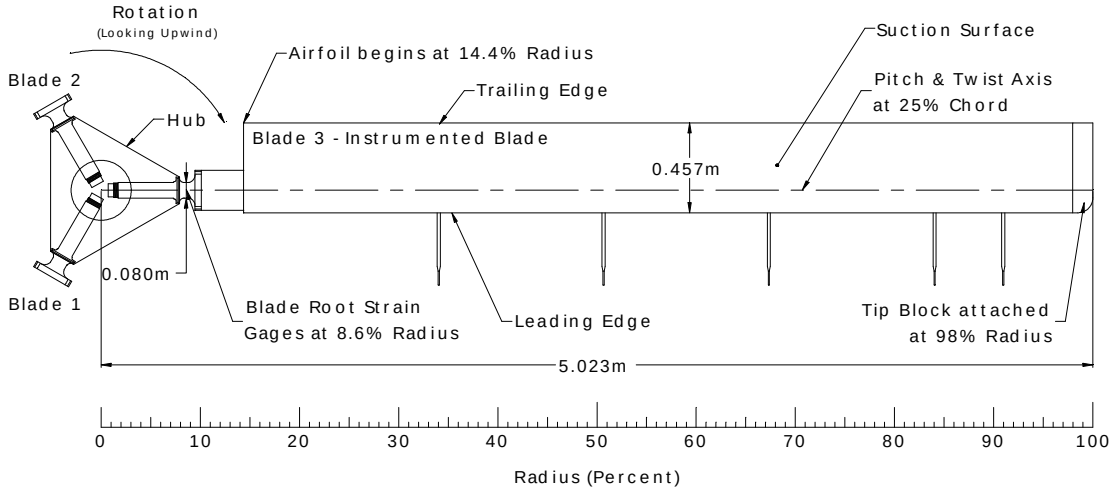

Figure 4. Twisted blade planform.

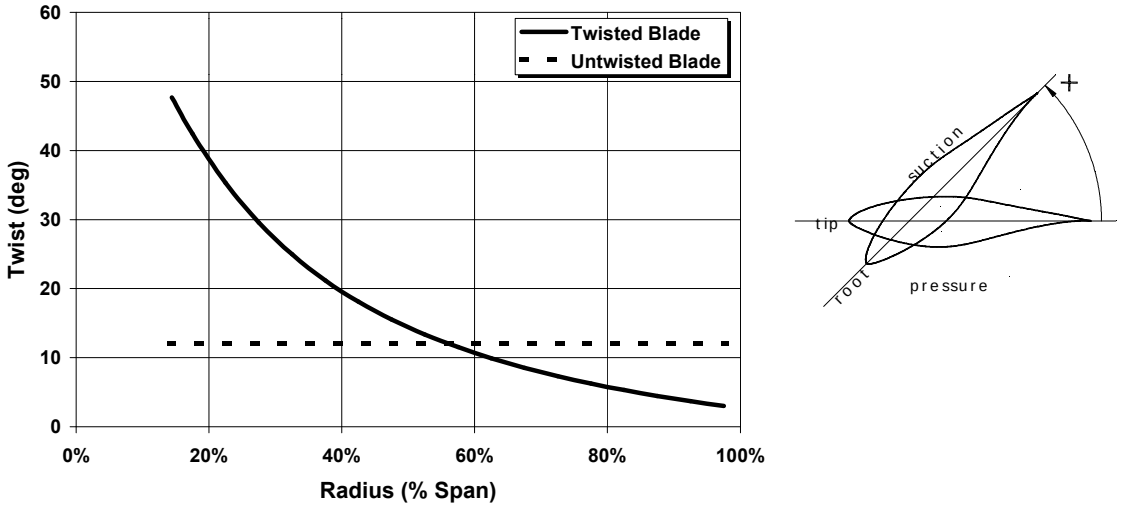

Figure 5. Blade twist distribution at the pitch setting used most frequently during experiment data acquisition: 12° for Phase II and 3° (at tip) for Phases III and IV

INSTRUMENTATION

Meteorological (MET) Towers

During Phase II, the inflow conditions were measured at three locations in the predominant upwind direction (292°): the north met tower, the local met tower, and the vertical plane array (VPA). The north met tower was 50 m tall and located 500 m upwind of the turbine. Large-scale atmospheric boundary-layer conditions were measured at this location in the form of wind speed and direction at four elevations (5 m, 10 m, 20 m, and 50 m), temperature at 5 m and at 50 m, and barometric pressure. Local inflow measurements were made 12 m upwind of the turbine on the VPA which is depicted in Figure 6. Two Rohn 45-G guyed met towers supported three cross-booms, where 11 prop-vane and 2 bi-vane anemometers measured inlet flow magnitude and direction. Eight of the prop-vane anemometers were arranged in a circle corresponding to 80% of the blade span at about hub height, 17 m. The remaining prop-vane anemometers were spaced evenly inside the circle. The two bi-vane anemometers were mounted outside the circle on the horizontal axis. Also located 12 m upwind of the turbine and 20 m to the north was the 16.8 m local met tower. Sonic anemometer measurements originated from this tower. Detailed discussion of the anemometry used in the Phase II portion of the experiment appears in Butterfield et al. (1992). Table 2 lists all of the channels related to measurements made on the Phase II met towers.

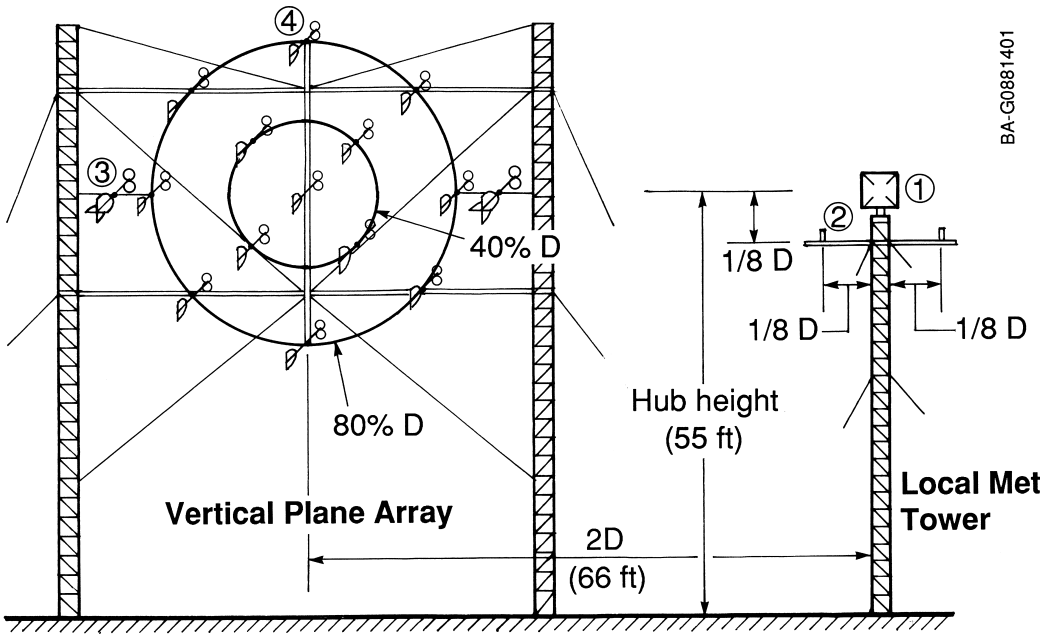

Item No.	Description	Quantity
1	U-V-W sonic anemometer	1
2	Ruggedized hot films	2
3	Bi vane anemometers	2
4	Prop vane anemometers	13

Figure 6. Phase II (Untwisted Blade) Meteorological Instrumentation. Elevation view looking downwind toward 112°. Meteorological instruments are 1.2 D (12 m) upwind of the turbine tower.

Table 2. Phase II (Untwisted Blade) Local Inflow Measurements

Channel	Channel ID	Description	Units
038	VPAWS1	VPA Prop Vane Speed WS-1 (12:00)	m/s
039	VPAWS2	VPA Prop Vane Speed WS-2 (1:30)	m/s
040	VPAWS3	VPA Prop Vane Speed WS-3 (3:00)	m/s
041	VPAWS4	VPA Prop Vane Speed WS-4 (4:30)	m/s
042	VPAWS5	VPA Prop Vane Speed WS-5 (6:00)	m/s
043	VPAWS6	VPA Prop Vane Speed WS-6 (7:30)	m/s
044	VPAWS7	VPA Prop Vane Speed WS-7 (9:00)	m/s
045	VPAWS8	VPA Prop Vane Speed WS-8 (10:30)	m/s
046	VPAWS9	VPA Prop Vane Speed WS-9 Hub Height	m/s
047	VPAWD9	VPA Prop Vane Direction WD-9 Hub Height	deg
048	VPAWS12	VPA Bi-Vane Speed WS-12 (3:00 @100%)	m/s
049	VPAWD12	VPA Bi-Vane Direction WD-12 (3:00 @100%)	deg
050	VPAWE12	VPA Bi-Vane Elevation WE-12 (3:00 @100%)	deg
051	VPAWS13	VPA Bi-Vane Speed WS-13 (9:00 @100%)	m/s
052	VPAWD13	VPA Bi-Vane Direction WD-13 (9:00 @100%)	deg
053	VPAWE13	VPA Bi-Vane Elevation WE-13 (9:00 @100%)	deg
054	VPAWS10	VPA Prop Vane Speed WS-10 (12:00 @40%)	m/s
055	VPAWS11	VPA Prop Vane Speed WS-11 (6:00 @40%)	m/s
102	LMSA17M	Sonic Anemometer Channel A	m/s*
103	LMSB17M	Sonic Anemometer Channel B	m/s*
104	LMSC17M	Sonic Anemometer Channel C	m/s*
300	NMWD5M	North Met Wind Direction 5 m	deg*
301	NMWS5M	North Met Wind Speed 5 m	m/s
302	NMWD10M	North Met Wind Direction 10 m	deg*
304	NMWD20M	North Met Wind Direction 20 m	deg
305	NMWS20M	North Met Wind Speed 20 m	m/s
306	NMWD50M	North Met Wind Direction 50 m	deg
307	NMWS50M	North Met Wind Speed 50 m	m/s
308	NMT5M	North Met Temperature 5 m	degC
309	NMDT	North Met Delta Temperature T50-T05	degC
310	BARO	Barometric Pressure	Pa

* These channels do not appear in all campaigns.

Inflow conditions were again measured directly upwind of the turbine during Phases III and IV, but the north met tower was not used. Instead, a taller local met tower was used to measure shear and stability near the turbine. Three met towers placed 1.5 D (15 m) upwind of the turbine supported multiple cup anemometers, bi-vane anemometers and one sonic anemometer. The cup anemometers provided more accurate wind speed measurements than the prop-vane anemometers used during Phase II because the cup anemometers have a higher frequency response and are not susceptible to gyroscopic effects. Temperature and barometric pressure measurements were also made. Figure 7 shows the three, instrumented, met towers. Phase III and Phase IV meteorological channel descriptions are shown in Table 3 and detailed instrumentation and wiring information is presented in Appendix B.

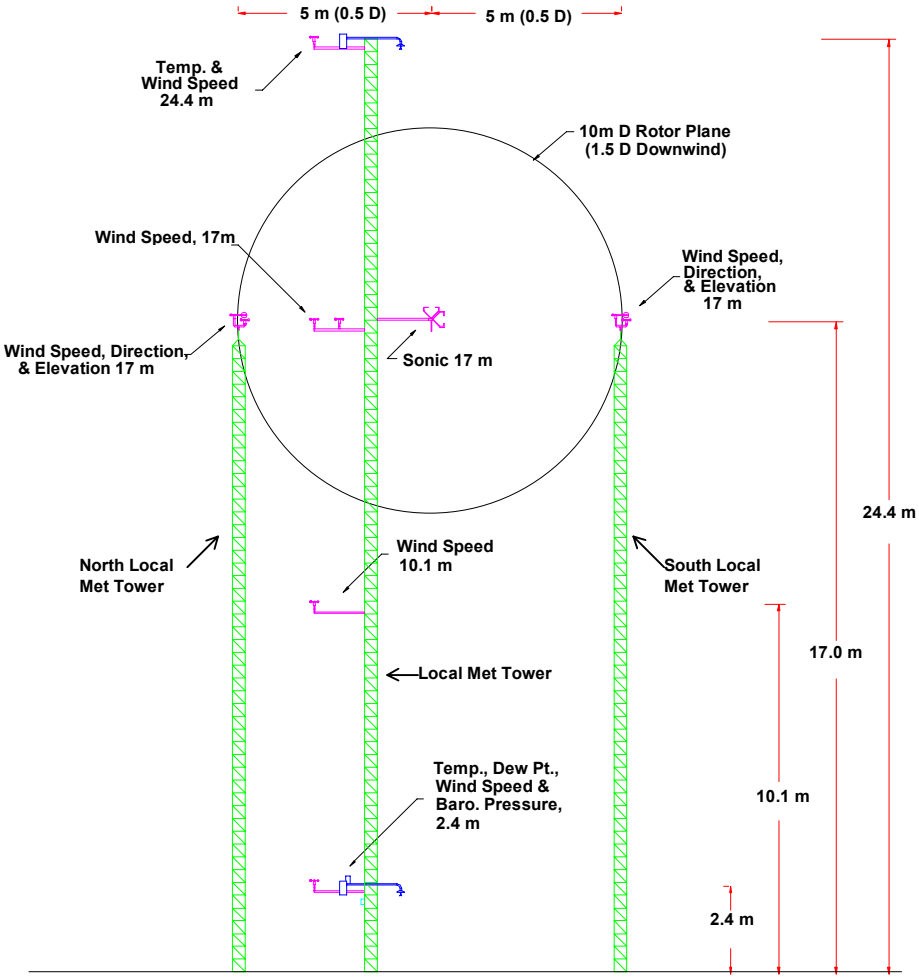

Figure 7. Phase III and Phase IV (twisted blade) meteorological instrumentation. Elevation view looking downwind toward 112°. Meteorological instruments are 1.5 D (15 m) upwind of the turbine tower.

Table 3. Phase III and Phase IV (Twisted Blade) Local Inflow Measurements

Channel	Channel ID	Description	Units
300	LMWS24M	Local Met Wind Speed 24.38 m	m/s
302	LMWS17M	Local Met Wind Speed 17.02 m (hub height)	m/s
304	LMWS10M	Local Met Wind Speed 10.06 m	m/s
306	LMWS2M	Local Met Wind Speed 2.4 m	m/s
308	NLMWS17M	N local Met Wind Speed 17.02 m (hub height)	m/s
310	NLMWD17M	N local Met Wind Direction 17.02 m (hub height)	deg
312	NLMWE17M	N local Met Wind Elevation 17.02 m (hub height)	deg
314	SLMWS17M	S local Met Wind Speed 17.02 m (hub height)	m/s
316	SLMWD17M	S local Met Wind Direction 17.02 m (hub height)	deg
318	SLMWE17M	S local Met Wind Elevation 17.02 m (hub height)	deg
320	LMT2M	Local Met Temperature 2.4m	degC
322	LMDT	Local Met Delta Temperature	degC*
322	LMT24M	Local Met Temperature 24.38 m	degC*
324	LMDP2M	Local Met Dewpoint 2.4m	degC
326	LMSU17M	Local Met Sonic Channel U 17.02 m	m/s
328	LMSV17M	Local Met Sonic Channel V 17.02 m	m/s
330	LMSW17M	Local Met Sonic Channel W 17.02 m	m/s
334	BARO	Barometric Pressure	Pascal

* These channels do not appear in all campaigns.

Pressure Measurements

Pressure Probes

A Kiel pitot probe attached to the local flow angle flag pictured in Figure 8 measured dynamic pressure during Phases II and III. The Kiel pitot probe configuration provides total pressure measurement over a wider range of angle of attack than conventional pitot probes. To prevent flow disturbance, the probe extended 0.64 m (0.62 m during Phase II) ahead of the leading edge along the chord line of the airfoil and was mounted 4% outboard of each primary pressure station (30%, 47%, 63%, and 80%). The probe was mounted at 86% span instead of 84% span during Phase II. To maximize the probes' effectiveness, the probe tips were bent about 20° below the chord line as shown in Figure 8, so the measurement range would coincide with the nominal operating angle of attack. Each probe was connected to a pressure transducer via 1.5875 mm outer diameter (0.6731 mm inner diameter) stainless steel tubing. A short piece of plastic tubing was used to join the tubes to the transducer. The probes measured the difference between the stagnation and reference pressures with less than 10% error for inflow angles between -40° and 40° (Huyer 1993). The channels associated with the Phase II probe pressure measurements appear in Table 16 with the stagnation pressure channels.

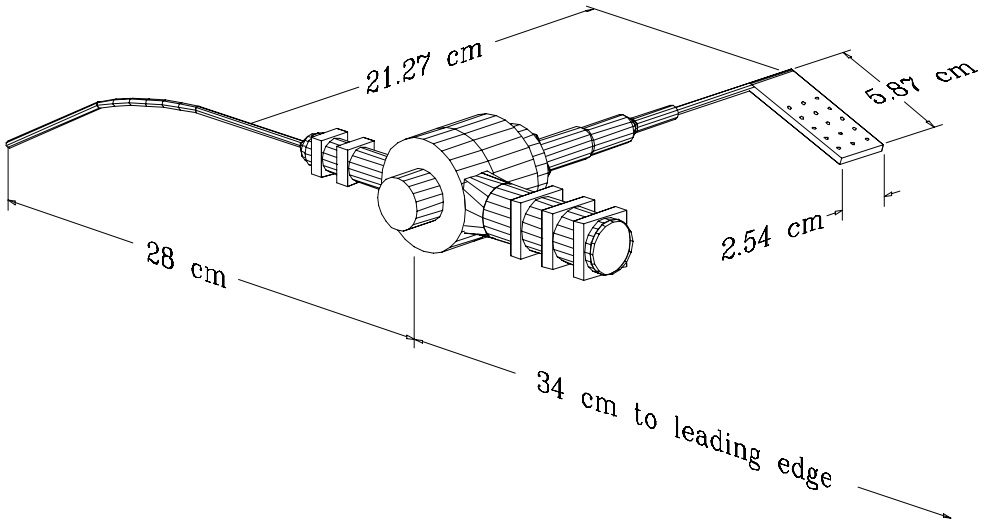

Figure 8. Local flow angle flag and total pressure probe assembly used during Phase II and Phase III.

During Phase IV the 5-hole probe shown in Figure 9 provided a dynamic pressure measurement 0.37 m ahead of the leading edge at an angle of 20° below the chord line. The 5-hole probes were mounted in the same locations as the pitot probes with the addition of one at 91% span. The pressure channels associated with each of the five holes are listed in Table 4. Each probe was calibrated in a wind tunnel with a 0.914 x 0.914 m (3 x 3 ft) cross-section. The probe was mounted in the center of the test section, and pressure data were acquired for angles of attack from -40° to 40°. The probe was then rotated 15° and tested for the same angle of attack range. This was done for roll angles of 0°, 15°, 30°, 45°, 60°, 90°, 120°, 135°, and 150°. The difference between the inboard and outboard pressures was normalized with the tunnel dynamic pressure to correspond with the span-wise flow angle. The difference in pressure between the upper (towards upper surface of the airfoil) and lower port measurements was normalized with the tunnel dynamic pressure in order to calibrate the local flow angle. The center port pressure normalized with the tunnel dynamic pressure provided the total pressure. These wind tunnel data were input to a neural network model to create surfaces for each of the three probe measurements for all five probes. The surfaces were implemented as look-up tables in the post-processing code. An iterative solution was developed to determine the probe total pressure measurement, and bi-linear interpolation was used to obtain all three measurements from their respective surfaces (Fingersh and Robinson 1997). The span-wise flow angle and local flow angle channels appear in Table 10 and the dynamic pressure measurements appear in Table 16. A single, 5-hole probe mounted at 91% span was tested during Phase III. This probe extended 0.34 m ahead of the leading edge of the blade and was aligned with the chord. As a result of the satisfactory performance, all of the flag devices were replaced with 5-hole probes for Phase IV testing.

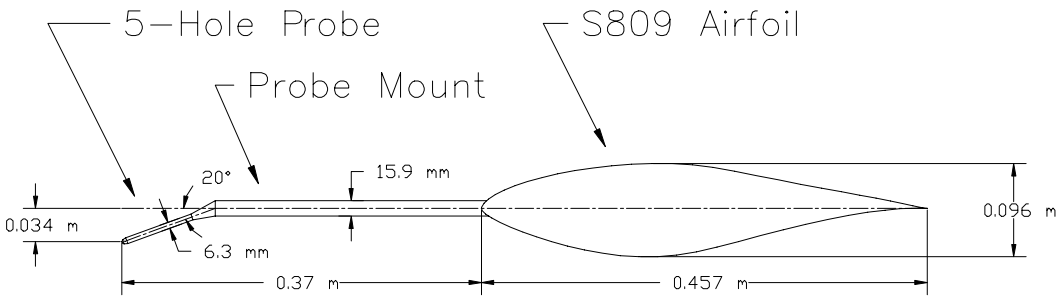

Figure 9. Blade mounted 5-Hole probe (During Phase III the test probe at 91% span extended 0.34 m in front of the blade aligned with the chord, not declined 20°).

Table 4. Phase III and IV 5-Hole Probe Pressures

Channel	Channel ID	Description	Units
052, 053, 152, 153, 252	5HC34, 5HC51, 5HC67, 5HC84, 5HC91, 5HC90*	5-hole Center Port 1 (34%, 51%, 67%, 84%, and 91% span)	Pa
054, 055, 154, 155, 254	5HL34, 5HL51, 5HL67, 5HL84, 5HL91, 5HL90*	5-hole Lower Port 2 (34%, 51%, 67%, 84%, and 91% span)	Pa
056, 057, 156, 157, 256	5HU34, 5HU51, 5HU67, 5HU84, 5HU91, 5HU90*	5-hole Upper Port 3 (34%, 51%, 67%, 84%, and 91% span)	Pa
058, 059, 158, 159, 258	5HO34, 5HO51, 5HO67, 5HO84, 5HO91, 5HO90*	5-hole Outboard Port 4 (34%, 51%, 67%, 84%, and 91% span)	Pa
060, 061, 160, 161, 260	5HI34, 5HI51, 5HI67, 5HI84, 5HI91, 5HI90*	5-hole Inboard Port 5 (34%, 51%, 67%, 84%, and 91% span)	Pa

* Phase III channel ID incorrectly lists the single 5-hole probe at 90% span

The probe was not rotated to the appropriate angle for one of the runs during the wind tunnel calibration of the probe that was mounted at 51% span,. This was not discovered until the first portion of Phase IV (data20-data112, slwrot4, and slwrot5) had been completely processed. New surfaces for the 51% span probe were generated using the data obtained from another probe at that particular roll angle. These new surfaces were implemented in the processing of Phase IV data obtained in 1997.

Pressure Taps

The most important, yet most difficult, measurements were the blade surface tap pressures. The quality of the aerodynamic performance coefficients depends on the accuracy of individual pressure tap measurements. Aerodynamic coefficients for a particular radial station resulted from the integrated value of the measured pressure distribution. The measurement approach was to install small pressure taps in the surface of the blade skin. Each opening was mounted flush to the airfoil surface. The flush profile was necessary to prevent the taps themselves from

disturbing the flow. Stainless steel tubes with an outer diameter of 1.5875 mm (0.6731 mm inner diameter), were installed inside the blade's skin during manufacturing to carry surface pressures to the pressure transducer. A short piece of plastic tubing (0.6731 mm inner diameter) joined the tubes to the transducers. To mitigate potential dynamic effects, total tubing length was kept less than 0.45 m (18 in) by mounting the pressure transducers inside the blade near the pressure tap locations. The taps were aligned along the chord (instead of being staggered) so that span-wise variations in pressure distributions would not distort measured chordwise distributions. As illustrated in Figure 10, the taps were concentrated toward the leading edge to achieve increased resolution in the more active areas of the pressure distributions.

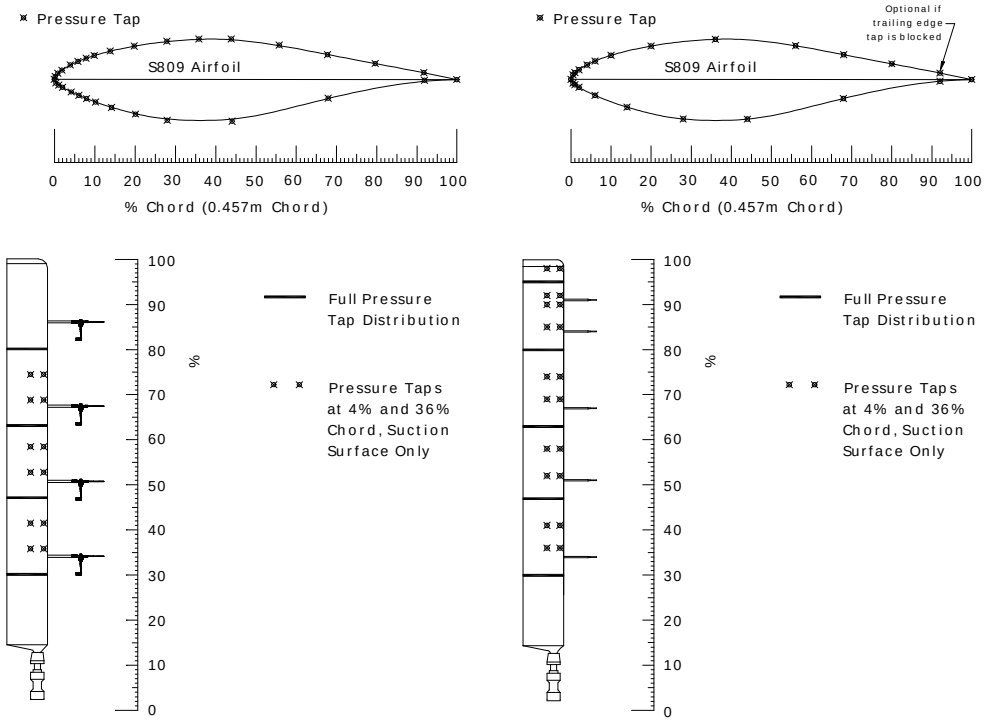

Figure 10. Configuration of Phase II (untwisted) instrumented blade and Phase IV (twisted) instrumented blade. During Phase III, the local flow angle flags were used at the four inboard flow angle stations, and a 5-hole probe was tested at 91% span. The pressure tap configuration was identical to that used during Phase IV.

The Phase II experiment used 28 of the 38 pressure taps at four primary radial locations: 30% span, 47% span, 63% span, and 80% span. Table 5 describes the pressure tap locations used during Phase II. During Phases III and IV, 22 of the 38 taps were instrumented at five primary span-wise locations: 30% span, 47% span, 63% span, 80% span, and 95% span. Pairs of taps at 4% chord and 36% chord were installed at various other intermediate span locations (36%, 41%, 52%, 58%, 69%, 74%, 85%, 90%, 92%, and 98%). These channels are listed in Table 6. The correlation between pressure tap number and airfoil chord location is shown in Table 7. Figure 10 depicts the blade layout for Phases II and IV. The Phase III blade layout differed from the Phase IV layout in that the local flow angle flag assemblies were mounted at the four inboard primary span locations instead of the 5-hole probes. Also the 5-hole probe mounted at 91% span was aligned with the chord line, not bent into the dominant flow direction as was done for the probes used during Phase IV.

Table 5. Phase II Pressure Tap Locations

Channel	Channel ID	Description	Units
002-029	Ptt63ccc	Surface Pressure Coefficients at 63% Span tt = Pressure Tap Number (1, 2, 4, 6, 8, 10, 11, 12, 13, 14, 15, 16, 17, 18, 19, 20, 21, 22, 23, 24, 25, 26, 28, 30, 32, 34, 36, 38)	Pa
124-151	Ptt80ccc	Surface Pressure Coefficients at 80% Span tt = Pressure Tap Number (1, 2, 4, 6, 8, 10, 11, 12, 13, 14, 15, 16, 17, 18, 19, 20, 21, 22, 23, 25, 26, 27, 28, 30, 32, 34, 36, 38)	Pa
200-224	Ptt30ccc	Surface Pressure Coefficients at 30% Span tt = Pressure Tap Number (1, 4, 6, 8, 10, 11, 13, 14, 15, 16, 17, 18, 19, 20, 21, 22, 23, 24, 25, 26, 28, 30, 31, 34, 36, 38)	Pa
229-256	Ptt47ccc	Surface Pressure Coefficients at 47% Span tt = Pressure Tap Number (1, 2, 4, 6, 8, 10, 11, 12, 13, 14, 15, 16, 17, 18, 19, 20, 21, 22, 23, 25, 26, 27, 28, 30, 32, 34, 36, 38)	Pa
000, 001, 030-032, 152-154, 225-227, 257	P18ss04U P11ss36U	Surface Pressure Coefficients at 36%, 41%, 52%, 58%, 69%, and 74% Span Pressure Tap Number (11, 18)	Pa

Table 6. Phase III and Phase IV Pressure Tap Locations

Channel	Channel ID	Description	Units
000-042 (even)	Ptt30ccc	Surface Pressure Coefficients at 30% Span tt = Pressure Tap Number (1, 4, 6, 8, 11, 13, 15, 17, 18, 19, 20, 21, 22, 23, 24, 25, 27, 31, 32, 34, 36,	Pa
001-043 (odd)	Ptt47ccc	Surface Pressure Coefficients at 47% Span tt = Pressure Tap Number (1, 4, 6, 8, 11, 13, 15, 17, 18, 19, 20, 21, 22, 23, 24, 25, 27, 31, 32, 34, 36,	Pa
100-142 (even)	Ptt63ccc	Surface Pressure Coefficients at 63% Span tt = Pressure Tap Number (2, 4, 6, 8, 11, 13, 15, 17, 18, 19, 20, 21, 22, 23, 24, 25, 27, 30, 32, 34, 36,	Pa
101-143 (odd)	Ptt80ccc	Surface Pressure Coefficients at 80% Span tt = Pressure Tap Number (1, 4, 6, 8, 11, 13, 15, 17, 18, 19, 20, 21, 22, 23, 24, 25, 27, 30, 32, 35, 36,	Pa
200-250 (even)	Ptt95ccc	Surface Pressure Coefficients at 95% Span tt = Pressure Tap Number (2, 4, 6, 8, 11, 13, 15, 17, 18, 19, 20, 21, 22, 23, 24, 25, 27, 30, 32, 34, 36,	Pa
44-51, 144-151, 244-250 (even)	P18ss04U P11ss36U	Intermediate surface Pressure Coefficients at 36%, 41%, 52%, 58%, 69%, 74%, 85%, 90%, 92%, and 98% Span Pressure Tap Number (11, 18) P118536U was inoperable.	Pa

Table 7. Pressure Tap Chord Locations

Pressure Tap Number	% chord	Surface	tt*	ccc*
1	100%	Trailing edge	01	100
2	92%	Upper	02	92U
4	80%	Upper	04	80U
6	68%	Upper	06	68U
8	56%	Upper	08	56U
10	44%	Upper	10	44U
11	36%	Upper	11	36U
12	28%	Upper	12	28U
13	20%	Upper	13	20U
14	14%	Upper	14	14U
15	10%	Upper	15	10U
16	8%	Upper	16	08U
17	6%	Upper	17	06U
18	4%	Upper	18	04U
19	2%	Upper	19	02U
20	1%	Upper	20	01U
21	0.5%	Upper	21	.5U
22	0%	Leading edge	22	000
23	0.5%	Lower	23	.5L
24	1%	Lower	24	01L
25	2%	Lower	25	02L
26	4%	Lower	26	04L
27	6%	Lower	27	06L
28	8%	Lower	28	08L
30	14%	Lower	30	14L
31	20%	Lower	31	20L
32	28%	Lower	32	28L
34	44%	Lower	34	44L
36	68%	Lower	36	68L
38	92%	Lower	38	92L

* See Tables 5 and 6

Based on tests performed in Phase I of the experiment, corrections to compensate for dynamic effects on pressure measurements caused by the pressure tap tubing were not applied to measured data sets (Butterfield et al. 1992). Effort was made to mitigate needed corrections by minimizing tubing diameter and keeping tubing length as short as possible. Gain amplifications and phase effects that occur as a function of tube size and length were measured. Results indicated that these effects were not significant up to a frequency of 40 Hz, and the measured pressure spectra of a typical data set showed no appreciable information above 40 Hz. Depending on data requirements, it would be possible to process data to remove the dynamic tubing effects. This may become necessary if, for example, a study of high-rate aerodynamic events were to be undertaken.

Pressure Transducer

The dynamic pressure varied significantly along the span because of rotational effects, so transducers with different measurement ranges were used. The nominal transducer ranges used during different test phases are listed below in Table 8. The transducers, Pressure Systems Inc. (PSI) model ESP-32, scanned port to port at 16,666 Hz and completed a scan of all pressure taps at 520.83 Hz. One transducer was used at each primary span location to measure up to 32 differential pressures at the blade surface pressure taps and each of the five ports of a 5-hole probe (local static pressure). These measurements were referenced to the pressure in one of the hub-mounted instrumentation boxes. Corrections were applied to account for the centrifugal force acting on the air column in the reference tube. Each transducer was installed inside the blade as close to the pressure taps as possible. These electronic scanner-type transducers provided remote calibration capability through a pneumatically operated valve. The capacity to purge all of the pressure taps with dry nitrogen was used periodically to prevent moisture or small particles from affecting the pressure measurements.

Table 8. Nominal, Full-scale, Pressure Transducer Measurement Ranges

	Phase II	Phase III and Phase IV
30% Span	± 2970 Pa (0.4 psi)	± 2488 Pa (10" H_2O)
47% Span	± 2970 Pa (0.4 psi)	± 2488 Pa (10" H_2O)
63% Span	± 8274 Pa (1.2 psi)	± 4977 Pa (20" H_2O)
80% Span	± 8274 Pa (1.2 psi)	± 10,342 Pa (1.5 psi)
95% Span		± 10,342 Pa (1.5 psi)

Differential pressures between the blade surface pressure and the hub reference pressure were measured by the ESP-32 pressure transducers. For all blade surface pressure measurements as well as probe pressure measurements, the common reference pressure source was the pressure inside one of the rotating instrumentation boxes on the hub which was assumed to be free stream static pressure. Each transducer located in the blade was connected to the reference source via a plastic 0.6731 mm inner diameter tube between the hub and the transducer. The hub-mounted instrumentation box was vented to the atmosphere through an orifice on the upwind side of the box. This resulted in a time constant of about 5-10 seconds, and provided a relatively stable pressure reference. During Phase III and the first season of Phase IV (1996), heaters in the instrumentation packages were thermostatically controlled to prevent condensation inside the boxes. When the heaters cycled on and off, the static pressure in the box changed significantly affecting all of the measured pressures. The portions of each campaign affected by the heaters are noted in Appendix D. During the second season of Phase IV data collection (1997), the heaters were turned off during data collection.

The hub-mounted instrumentation boxes used during Phases III and IV differed from those used during Phase II. As described above, the Phase III and IV box reference pressure was vented to the atmosphere on the upwind side. During Phase II, the box was sealed as tightly as possible. Comparison of measured blade dynamic pressure versus wind speed estimated dynamic pressure has shown that the reference pressure in the box during Phase II was slightly higher than free stream static pressure. However, similar comparisons in the Phase III and IV data showed that the box reference pressure varied significantly from static pressure. Subsequent direct measurement confirmed the result. Therefore, all pressure measurements should be corrected for this reference pressure offset. This correction is described in the "Reference Pressure Correction" section below, and will be further addressed in subsequent reports.

Because of the rotation of the reference pressure line, centrifugal forces acting on the column of air contained in the tube change the pressure along the radius of the blade. Each measurement was corrected for centrifugal force effects and normalized with the blade stagnation pressure as described in the Engineering Unit Conversion section that follows. No correction for hydrostatic pressure variation has been applied, but one has been suggested by Corten, 1998.

Pressure System Controller (PSC)

Remote control of ESP-32 pressure transducer calibration, scanner addressing, and demultiplexing of the analog multiplexed signals were performed by the PSC, a hub-mounted microprocessor control unit designed by NREL (Butterfield et al. 1992). The PSC was completely redesigned from Phase II to Phase III to improve the accuracy and the user interface. Currently up to 155 pressure channels may be processed simultaneously. All pressure ports were scanned at 520.83 Hz. The objective was to provide 100 Hz bandwidth frequency response to enable study of dynamic stall behavior on the rotating wind turbine blade.

Once the PSC scanned the pressure transducers, the samples were digitized, synchronized, and passed to the pulse code modulation (PCM) encoder. The PCM system multiplexed 62 channels of data into one digital data stream which was conducted through a single coaxial cable. Rotor data were encoded into three PCM streams which were passed over slip rings to the control building and were recorded on optical disk for subsequent processing.

The PSC pneumatic control valves and ramp calibration sequence is discussed in the Phase I report (Butterfield et al. 1992) and summarized in Appendix B. The only changes between Phase II and later phases were that a more accurate calibration reference pressure was used, and calibrations were automated by a computer-controlled processing system.

Local Flow Angle (LFA) Transducers

Geometric angle of attack (AOA) measurements are fairly easy to make in a wind tunnel where the air flow is precisely controlled. It is significantly more difficult to quantify AOA on a rotating blade in the field. This is in part because of widely varying environmental factors such as dynamic inflow, turbulence, wind shear, and yawed operation. It is additionally complicated by blade upwash due to bound vorticity, AOA measurement device effects on airfoil performance, and 3-D flow effects in the rotating environment. Based on these considerations, it is highly unlikely that a measurement parameter equivalent to 2-D AOA can be made in the 3-D operating environment. Therefore, LFA measurements were made instead as an attempt to provide an approximation or estimation of the inflow angle.

The LFA sensor illustrated in Figure 8 was developed by NREL for this purpose (Butterfield et al. 1992) and was used in Phase II and Phase III tests. It consisted of a lightweight, rigid flag that aligned itself with the local flow. During Phase II tests, a commercial rotary position sensor mounted in a custom housing measured the flag angle within ±1.0° accuracy over the range of -20° to 40°. The analog signals generated were sent to the hub, multiplexed, and recorded with the other signals by the data acquisition system. This analog position encoder was replaced with a digital resolver during Phase III testing to increase measurement accuracy. The flag extended 36 cm (34 cm during Phase II) ahead of the leading edge and was aligned with the pressure taps. The sensor was attached to the blade 4% outboard of the four primary pressure stations (30%, 47%, 63%, and 80%) in order to minimize flow disturbances on the blade near the pressure taps.

During Phase II the flag sensor was actually mounted at 86% span measuring a local flow angle at 82% span instead of 80% span. However, in Phase II testing, this local flow angle is associated with the 80% span pressure tap location. Processing of the data revealed that during Phase II the flag at 47% span did not work properly for most of the duration of testing so it was removed from the processed data files. The following table describes the local flow angle measurements for Phase II and Phase III. Additional information concerning the digital resolver used during Phase III may be found in Appendix B.

Table 9. Phase II and Phase III Local Flow Angle Measurements (Flag)

Channel	Channel ID	Description	Units
034 (II), 249 (III	80LFA	80% Span Local Flow Angle (Flag)	deg*
035 (II), 247 (III	63LFA	63% Span Local Flow Angle (Flag)	deg
245 (III)	47LFA	47% Span Local Flow Angle (Flag)	deg
037 (II), 243 (III	30LFA	30% Span Local Flow Angle (Flag)	deg

* Actually measured LFA at 82% span during Phase II.

During Phase III, a 5-hole probe was mounted 4% inboard of the 95% span pressure station in order to test this device for measuring local flow angle. The probe was designed to measure angles in the range ±45°. Because the probe was mounted parallel to the chord line of the blade, it was not within this prescribed measurement range for many operating conditions. For this reason, these data should be regarded with discretion, but the test did prove that the five hole probe provided greater dynamic response than the flag which is necessary in studying dynamic stall (Fingersh and Robinson 1997). Therefore all of the flag sensors were replaced with five hole probes during Phase IV testing. The probes, depicted in Figure 9, extended 37 cm ahead of the leading edge at an angle about 20° below the chord line and measured local flow angles over the range from -15° to 55°. They were mounted 4% span outboard of the primary pressure stations except at the 95% pressure tap station where the probe was mounted 4% span inboard. The local flow angle measurement from the probe is no longer aligned with the full-chord pressure measurements as was the local flow angle measured with the flag. Thus blade twist and rotational effects are introduced. In addition to the local flow angle, the 5-hole probes used in Phase IV provided measurement of the span-wise flow angle. The following table describes the local flow angle measurements made during Phase IV.

Table 10. Phase IV Local Flow Angle Measurements (5-Hole Probe)

Channel	Channel ID	Description	Units
853	5HP34A	5Hole 34% Local Flow Angle (Angle of Attack)	deg
856	5HP51A	5Hole 51% Local Flow Angle (Angle of Attack)	deg
859	5HP67A	5Hole 67% Local Flow Angle (Angle of Attack)	deg
862	5HP84A	5Hole 84% Local Flow Angle (Angle of Attack)	deg
865	5HP91A	5Hole 91% Local Flow Angle (Angle of Attack)	deg
854	5HP34F	5Hole 34% Spanwise Flow Angle	deg
857	5HP51F	5Hole 51% Spanwise Flow Angle	deg
860	5HP67F	5Hole 67% Spanwise Flow Angle	deg
863	5HP84F	5Hole 84% Spanwise Flow Angle	deg
866	5HP91F	5Hole 91% Spanwise Flow Angle	deg

Strain Gages and Accelerometers

Blade, tower, rotor, and yaw loads were measured with strain gages during Phase II testing. Six span-wise locations on the instrumented blade, root (8% span), 20% span, 40% span, 50% span,

70% span, and 90% span, were instrumented with strain gages to measure blade flap-wise bending while two locations, root (8% span) and 50% span, were instrumented to measure edge bending. Blade pitching moment (blade torsion) was measured at the root (8% span), 50% span and 70% span. Root flap and edge bending moments were also measured on the other two blades. Bending of the low speed shaft in two orthogonal planes was measured as well as the low speed shaft torque. Loads in the non-rotating environment were also measured. Gages were mounted on two tower bending axes at the point just above the guy wire attachment. These gages were oriented to measure bending parallel and perpendicular to the direction of the prevailing wind. Gages were mounted on the arm of the yaw brake to measure yaw moment when the yaw brake was engaged. All load measurements corresponding to Phase II tests are listed in Table 11. Estimates of thrust and torque derived from aerodynamic forces as described in the Engineering Unit Conversion section were also included in Table 11.

Table 11. Phase II (Untwisted Blades) Load Measurements

Channel	Channel ID	Description	Units
57	YAWMOM	Yaw Moment	N-m
58	TBEWAX	Tower Bending about East-West Axis (X)	N-m
59	TBNSAY	Tower Bending about North-South Axis (Y)	N-m
105	B3ARFB	Strain Blade 3A, Root Flap Bending	N-m
106	B3BRFB	Strain Blade 3B, Root Flap Bending (duplicate)	N-m
107	B1RFB	Strain Blade 1, Root Flap Bending	N-m
108	B2RFB	Strain Blade 2, Root Flap Bending	N-m
109	B320FB	Strain Blade 3, 20% Flap Bending	N-m
110	B340FB	Strain Blade 3, 40% Flap Bending	N-m
111	B350FB	Strain Blade 3, 50% Flap Bending	N-m
112	B370FB	Strain Blade 3, 70% Flap Bending	N-m*
113	B390FB	Strain Blade 3, 90% Flap Bending	N-m
114	B3AREB	Strain Blade 3, Root Edge Bending	N-m
115	B320EB	Strain Blade 3, 20% Edge Bending	N-m
116	B350EB	Strain Blade 3, 50% Edge Bending	N-m
117	70TQ	70% Blade Torque	N-m*
118	RTTQ	Root Torque (link)	N-m
119	50TSN	Blade 3 Torsion at 50% Span	N-m
120	LSSXXB	Strain X-X LSS Bending	N-m
121	LSSYYB	Strain Y-Y LSS Bending	N-m
122	LSSTQA	Strain LSS Torque A	N-m
123	LSSTQB	Strain LSS Torque B (duplicate channel)	N-m
813	EAEROTH	Thrust	N
814	EAEROTQ	Torque	N-m

* These channels do not appear in all campaigns.

Similar measurements were made during Phase III and IV testing periods. Flap and edge bending moments were recorded from strain gages mounted at the root (8.6% span), 25%, and 60% span on the instrumented blade. Flap and edge bending measurements were acquired at the root of the other two blades, and low speed shaft bending in two planes as well as low speed shaft torque measurements were also obtained. There were no pitching moment measurements made in either of these phases of the experiment. Instead of measuring tower bending with strain gages, accelerometers were placed in the nacelle to determine yaw, pitch, and fore-aft motion. Accelerometers were also used in the tips of each blade to measure acceleration in the flap and edge directions. During Phase IV, strain gages were used to measure yaw moment when the yaw brake was applied. A relatively constant yaw angle and non-zero, fluctuating, yaw moment

indicates the yaw brake was engaged during data acquisition. These measurements are listed in Table 12, and a description of the instrumentation is presented in Appendix B.

Table 12. Phase III and Phase IV (Twisted Blade) Load Measurements

Channel	Channel ID	Description	Units
201	B1ACFL	Accelerometer Blade 1-Flap	m/s^2*
203	B1ACED	Accelerometer Blade 1-Edge	m/s^2*
205	B2ACFL	Accelerometer Blade 2-Flap	m/s^2*
207	B2ACED	Accelerometer Blade 2-Edge	m/s^2*
209	B3ACFL	Accelerometer Blade 3-Flap	m/s^2*
211	B3ACED	Accelerometer Blade 3-Edge	m/s^2*
215	B325FB	Strain Blade 3 25% Flap Bending	N-m*
217	B325EB	Strain Blade 3 25% Edge Bending	N-m*
219	B360FB	Strain Blade 3 60% Flap Bending	N-m*
221	B360EB	Strain Blade 3 60% Edge Bending	N-m*
225	B1RFB	Strain Blade 1 Root Flap Bending	N-m*
227	B1REB	Strain Blade 1 Root Edge Bending	N-m*
229	B2RFB	Strain Blade 2 Root Flap Bending	N-m
231	B2REB	Strain Blade 2 Root Edge Bending	N-m
233	B3RFB	Strain Blade 3 Root Flap Bending	N-m
235	B3REB	Strain Blade 3 Root Edge Bending	N-m
237	LSSXXB	Strain X-X LSS Bending	N-m
239	LSSYYB	Strain Y-Y LSS Bending	N-m
241	LSSTQ	Strain LSS Torque	N-m
336	NAACYW	Nacelle Accelerometer Yaw	m/s^2
338	NAACFA	Nacelle Accelerometer Fore-Aft	m/s^2*
340	NAACPI	Nacelle Accelerometer Pitch	m/s^2
342	NAYM	Nacelle Yaw Moment	N-m*
813	EAEROTH	Thrust	Nt
814	EAEROTQ	Torque	Nt-m

* These channels do not appear in all campaigns.

During all phases of testing, strain gages measuring root flap and edge loads were applied to the steel pitch shaft adjacent to the blade attachment location. The pitch shaft was reduced to a uniform, cylindrical, 80 mm diameter at 8.6% (8% for Phase II) span, the location where the strain gages were applied. The uniform, cylindrical region eliminates geometry effects to facilitate accurate measurement of flap and edge bending moments. This cylindrical section of the blade root is illustrated in Figure 4 as well as in Appendix B.

Strain gages on the instrumented blades consisted of four active gage elements mounted inside the fiberglass blade skin. The gages were installed inside the skin during the blade manufacturing process to preserve the exterior airfoil shape and surface smoothness. The strain gages were positioned carefully to minimize flap-wise and edge-wise cross talk. A maximum of 4% cross talk was measured during the blade pull and strain gage calibration tests (Butterfield et al. 1992). These cross-channel interference effects were not considered significant, and corrections were not applied to the data.